ORIGINAL ARTICLE

The effect of Ganges river basin irrigation on pre-monsoon rainfall

J. K. Fletcher[1,2] | **C. E. Birch**[1] | **R. J. Keane**[1,3] | **C. M. Taylor**[4] | **S. S. Folwell**[4]

[1]School of Earth and Environment, University of Leeds, United Kingdom

[2]National Centre for Atmospheric Science, University of Leeds, United Kingdom

[3]UK Met Office, United Kingdom

[4]Centre for Ecology and Hydrology, Wallingford, United Kingdom

Correspondence
J. K. Fletcher, 71-75 Clarendon Road, University of Leeds, LS2 9PH, United Kingdom
Email: j.k.fletcher@leeds.ac.uk

Funding information
Newton Fund, WCSSP India WP2 Lot 3; Newton Fund, WCSSP India WP2 Lot 4; NERC, University of Leeds, NE/L013843/1; NERC, Centre for Ecology and Hydrology, NE/L013819/1

The first extended experiment studying the effect of irrigation on pre-monsoon rainfall in India using a high resolution convection permitting model has been carried out. This study includes both short (3 days) experiments and month-long free-running simulations, enabling investigation of the effect of irrigation under constrained and unconstrained synoptic conditions.

In the pre-monsoon, it is found that irrigation increases rainfall, in contradiction to previous studies using coarse models with parameterised convection over the monsoon season. Intriguingly, the rainfall increase found in the high resolution model mostly does not occur on the irrigated region, but on the mountains near the irrigation. This is because irrigation, which occurs in low-lying regions, enhances the mountain-valley flows leading to enhancement of diurnally-driven orographic rainfall. Because Ganges basin irrigation occurs near mountains that already have some of the highest rainfall rates in the world, and which are subject to flash flooding and landslides, this has significant implications for hazards in mountainous regions during the pre-monsoon and early monsoon period.

KEYWORDS
monsoon, India, irrigation, convection, precipitation

1 | INTRODUCTION

Northern India, particularly the Ganges basin, has some of the strongest precipitation-soil moisture coupling in the world (Koster et al., 2004). Understanding how atmospheric circulation and rainfall patterns respond to and feed back on irrigation patterns is therefore essential to improving our physical understanding and prediction of the South Asian monsoon. The Ganges River catchment plain supports roughly 400 million people on 1 million square km of land (Islam, 2006). This river catchment is highly managed, with more than half of the land equipped for irrigation (Siebert and Scanlon, 2015), generating a profound perturbation on the surface conditions. Douglas et al. (2006) estimate that irrigation produces a 17 % increase of surface latent heat fluxes over India compared to pre-agricultural times, and Lee et al. (2009) found statistically significant increases in surface latent heat fluxes in the late 20th Century which were associated with increases in the spatial extent of irrigation. (Niyogi et al., 2010) used causal data analysis methods on satellite retrievals of normalised differential vegetation index and suggested that pre-monsoon increases in vegetation led to decreases in monsoon rainfall. However, irrigation is not considered in weather and climate models, and Saeed et al. (2009) attributed a long-standing warm bias over the South Asian heat low region in many GCMs to the lack of representation of irrigation in the Indus river basin.

Observational studies (Douglas et al. 2006, Lee et al. 2009) suggest the importance of irrigation, but this must be disentangled from other anthropogenic forcings and internal variability. This separation is somewhat simpler in a modelling framework (see Shukla et al., 2013). Previous modelling studies of the effects of irrigation in India have used coarse resolution general circulation models (GCMs). These studies have found that large scale land surface cooling due to widespread irrigation weakened the monsoon circulation and reduced rainfall over central India (Saeed et al. 2009; Puma and Cook 2010; Cook et al. 2014; Chou et al. 2018) and delayed the monsoon onset by about a week (Guimberteau et al., 2011). These studies have attributed the surface cooling to evaporation (Puma and Cook 2010), increases in cloud cover (Sacks et al., 2008), or both (Cook et al. 2014; Chou et al. 2018). Shukla et al. (2013) argued that irrigation, combined with global surface temperature increases, is acting to reduce interannual variability in the Indian summer monsoon.

While it is reasonable to expect that the continental-scale circulation response to land surface temperature changes would be well-represented in a GCM, at least qualitatively if not quantitatively, there is less confidence that GCMs will produce the correct rainfall response, both to the large scale circulation changes and to the local scale changes in surface properties, particularly when convection is parameterized. Taylor et al. (2013) found that a weather forecasting model (run at higher resolution than the GCM studies discussed above) with parameterized convection failed to reproduce the observed relationship between soil moisture heterogeneity and convection in the Sahel: the model favoured convection over wet soils when observations of this environment – as well as those of nortwestern India – show that convection over wet soil is suppressed (Taylor et al. 2012; Barton et al. 2019). However, when Taylor et al. (2013) turned off deep convective parameterization, the same model reproduced the correct soil-moisture-precipitation feedback even at the relatively coarse horizontal resolution of 12 km. These results suggest that high resolution convection permitting models can uncover important aspects of the relationship between irrigation and monsoon rainfall, particularly the aspects that are driven by local convective and mesoscale processes and how those processes respond to surface forcing. While some regional modelling studies have been done (e.g., Douglas et al., 2009; Tuinenburg et al., 2014), these are still relatively coarse resolution and have parameterised convection.

In this paper, we make use of recent advances in high resolution convection permitting atmospheric modelling to study the effect of irrigation on mesoscale circulations and associated rainfall patterns over northern India. This paper is the first to our knowledge to use convection permitting models to examine the effects of irrigation over India.

2 | DATA AND METHODS

2.1 | Simulations

As explained below, our study was carried out for the pre-monsoon period in the Gangetic Plain region, so we show the mean circulation in that period in Figure 1. While there are large differences in both circulation and rainfall over the west coast of peninsular India, the Bengal region, and Myanmar, the monsoon onset in northern India typically does not arrive until later in June and the circulation and rainfall in both May and June are fairly similar to each other. Over the IGP region low level northwesterlies prevail except along the foothills of the Himalayas, where the winds blow southeasterly as the monsoon trough develops. Most rainfall over the north Indian monsoon core zone (Rajeevan et al., 2010) falls as isolated convective showers rather than as part of synoptic systems such as monsoon lows, which provide the bulk of rainfall to this region during the monsoon season proper (Hunt and Fletcher, 2019).

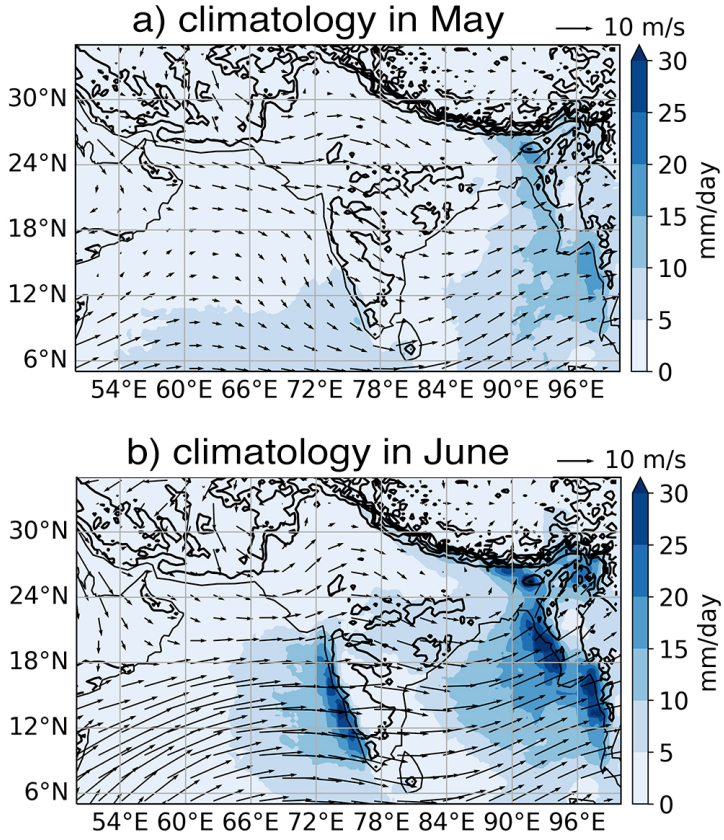

FIGURE 1 Mean 10m surface winds from ERA5 (Hersbach et al., 2020) and rainfall from GPM IMERG (Huffman et al., 2015) in May and June for the South Asian region.

We carried out simulations with the UK Met Office Unified Model (MetUM), with a horizontal resolution of 4.4 km and with the deep convection parametrization switched off. These simulations were over a regional domain covering

South Asia from 5°N to 35°N and from 50°E to 100°E, as illustrated in Figure 1. The regional model was driven on the boundaries by analyses and short-range simulations from the global MetUM (GA6.1/GL6.1): 6-hour global simulations were executed every 6 hours, starting from the Met Office operational analyses, to provide boundary conditions that were updated every hour. The regional simulations were initialised using the global analysis (downscaled to 4.4km) only once at the start so that, other than the forcing at the boundaries, the circulation within the regional domain was able to develop internally for the duration of each simulation. The regional model is described by Stratton et al. (2018) and Woodhams et al. (2018). This was applied over India by Martin et al. (2020), and the same setup is used in this study, except for the use of specially produced soil moisture ancillary files, as described in Section 2.2. We carried out two basic types of simulation, described below.

The first type of simulation was a continuously-run experiment over the month of June 2012, prior to the local onset for most of northern India. The circulation within the domain was able to develop internally for the duration of the simulation. We chose the pre- and early monsoon period because we expect that to be the time during which the effects of irrigation are strongest, because isolated convective showers dominate and convection is less organised by the large scale circulation than after monsoon onset, and because unirrigated soil is drier than during the monsoon, increasing the contrast between irrigated and unirrigated soil. The relatively clear sky conditions also make satellite-based estimates of where irrigation is occurring more accurate. For this simulation type, we carried out a control experiment and an irrigation experiment. The method used to represent irrigation is described in Section 2.2.

In order to cleanly separate the effect of irrigation from the model's synoptic internal variability, we also generated and analysed a suite of ten non-overlapping three-day simulations, in which the large scale forcings were constrained. These simulations were carried out over synoptically undisturbed periods in May and June 2016, prior to the onset of the monsoon in northern India. We focused on undisturbed times because synoptic scale organisation of rainfall as happens in, e.g., a monsoon low pressure system will at least partly mask the local effects of irrigation. As with the month-long simulation, we carried out control and irrigated experiments for each period simulated. In all figures below, the first day of each three day simulation was excluded unless stated otherwise, ~~allowing~~ both atmospheric and soil moisture spin-up.

As will be shown below, the month-long simulation and the three-day simulations (hereafter referred to as the long and short simulations) compliment each other: the short simulations ensure that we capture the synoptically-constrained response to irrigation, while the long simulation demonstrates that the full effect of irrigation takes time to develop and feeds back on the synoptic scale circulation (note that the large scale circulation is constrained by the boundary conditions). However, the long simulation was a preliminary study, with an unrealistically large soil moisture perturbation applied in the irrigation experiments. Therefore most of our analysis focuses on the short simulations.

2.2 | Soil moisture perturbations

As the MetUM does not currently model irrigation explicitly we introduced it through the soil moisture ancillary files. Soil moisture ancillary files were created for both the control simulation and the irrigation perturbations in the two sets of simulations. The control soil moisture for the month long simulation was produced by running a land surface model (JULES) offline forced with WFDEI (Weedon et al., 2011) at 0.5 degree resolution from the 2009-2014 mean soil moisture until equilibrium soil moisture was reached. The mean daily soil moisture was regridded to the coupled model resolution.

For the irrigation scenario the soil moisture was adjusted as follows. Irrigated areas were identified from pre-monsoon climatology of land surface temperature (LST) derived from the MODIS Terra satellite (Collection 5). We used clear-sky observations from the 1030 local time overpass for year 2003 to 2015 to produce a climatology of

LST at the 1 km resolution which was then regridded to the metUM resolution. This method offers simple objective identification of irrigation, including some measure of the degree of irrigation occurring. Our method suggests far more irrigation occurring in the lower Gangetic plain than was used during the pre-monsoon period by Chou et al. (2018). However, this method does not work well for high elevations, and so we limit our study to the low-lying Gangetic plain and do not represent Indus river region irrigation.

Three LST temperature thresholds were identified corresponding to irrigation in the Gangetic plain: fully irrigated below 313 K, partially irrigated between 313 K and 319 K, and not irrigated above 319 K. For grid boxes identified as fully irrigated soil moisture was set to just below the saturated level. Partially irrigated grid boxes with LST between 319 K and 313 K were prescribed a soil moisture between the mean value and just below saturation varying linearly with LST; grid boxes with LST above 319 K were unchanged.

The soil moisture ancillaries for the forecast runs were created following broadly similar steps, but they were altered to provide a more realistic modelled surface temperature distribution across irrigated areas and include more realistic spatial patterns of 2016 soil moisture by utilising the subsequently available gridded daily rainfall product (Mitra et al., 2009). This regional rainfall dataset combines satellite observations with daily gauged records and has the advantage of being at a 0.25 degree spatial resolution from October 2015 onwards. We created a new forcing dataset for the offline JULES runs by merging the gridded daily rainfall (Mitra et al., 2009) with the 3-hourly GLDAS2.1 NOAH reanalysis dataset on a 0.25 degree resolution (Rodell et al., 2004; Beaudoing and Rodell, 2016). The new soil moisture ancillary was spun up with just one year of forcing running from October 2015 to October 2016 to produce the quasi-equilibrium soil moisture.

Analysis of modelled LSTs obtained from the monthly simulations showed a strong cool bias corresponding with the partially irrigated grid boxes. This resulted from soil moisture in the top model soil layer being too readily available for bare soil evaporation and dominating grid box evaporation leading to too strong cooling. In the second iteration (for the short simulations) the soil moisture was increased ~~to~~ only to the soil critical point such that transpiration would not be water limited but reducing the strength of the bare soil evaporative signal.

2.3 | Other methods

Prior to plotting in maps, the data was smoothed using the python scipy package's Gaussian filter module, with sigma values ranging from 1-6. The statistical significance of differences in rainfall between the control and irrigation simulations were tested with the scipy package's ranksums module, employing a non-parametric test due to the non-Gaussian distribution of rainfall.

3 | RESULTS

3.1 | Mean differences

The effect of irrigation on mean rainfall and large scale circulation in the experiments is shown in Figure 2. In both the month-long simulation and the mean of the short simulations, irrigation weakens the monsoon trough in north-east India and Bangladesh while mostly increasing rainfall. The effect is much more pronounced in the month-long experiments, where the difference in mean sea level pressure (MSLP) between the control and irrigation experiments steadily increased over the course of the month, as shown in Figure 3. This suggests that, had these simulations been carried out over a full monsoon season, irrigation could have substantially delayed the monsoon onset in northern India, as seen in the previously mentioned GCM studies, even as irrigation increased pre-monsoon rainfall.

The rainfall response to the irrigation changes is much greater in the long run than in the short run, but it is unclear whether this is due to the length of the simulation or the magnitude of the forcing. To explore this further, we examine time series of rainfall and a few surface variables over the monsoon trough region in Figures 3 and 4.

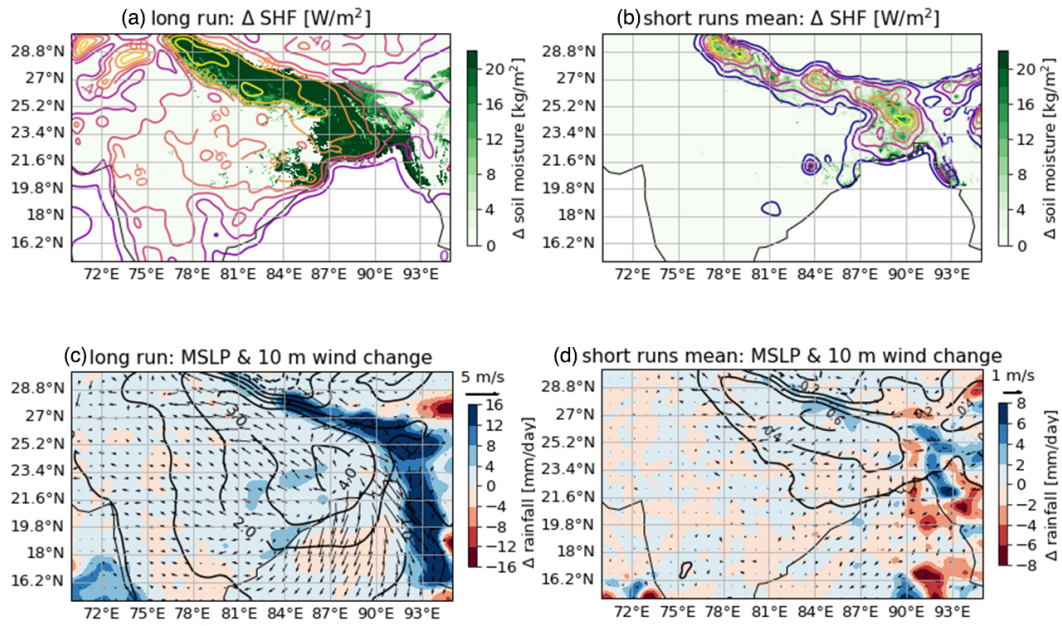

FIGURE 2 The surface perturbation (top row) and change in rainfall and circulation (bottom row) in the long (left) and short (right) irrigation experiments. In all panels, the difference between irrigation and control simulations are shown. Δ SHF is the change in surface sensible heat flux (positive up) and MSLP is the pressure at mean sea level in hPa. The contour interval is 20 W/m^2 in (a) and 5 W/m^2 in (b). Panels (b) and (d) show the means of the ten short simulations.

Figure 3 shows the time scale over which the long simulation control and irrigation experiments become substantially different from each other. For reference, the mean sea level pressure (MSLP) in ERA5 (Hersbach et al., 2020) and the rainfall from GPM IMERG (Huffman et al., 2015) is also shown. Given the model's freedom to evolve synoptically, we do not expect day-to-day rainfall agreement and only show IMERG to give a sense of the overall rainfall bias in the model. The irrigation experiment has both MSLP closer to ERA5 and rainfall closer to IMERG than control, but this does not necessarily mean that lack of irrigation is the cause of the low MSLP and dry biases in the control experiment. The first day has been excluded due to rapid adjustments in MSLP and rainfall that occur on that day. From day two there is already a mean difference in MSLP of about 1 hPa between control and irrigation over the entire monsoon trough region, with a corresponding reduction of surface sensible heat fluxes in excess of 50 W/m^2 in the irrigation experiment. However, the rainfall difference between the two experiments is small until about day five of the simulation, when the irrigation simulation begins to rain systematically more than the control experiment, with corresponding increases in the difference in MSLP and surface sensible heat fluxes.

The effects seen in the month-long runs also appear in the mean of the short simulations, but they are less

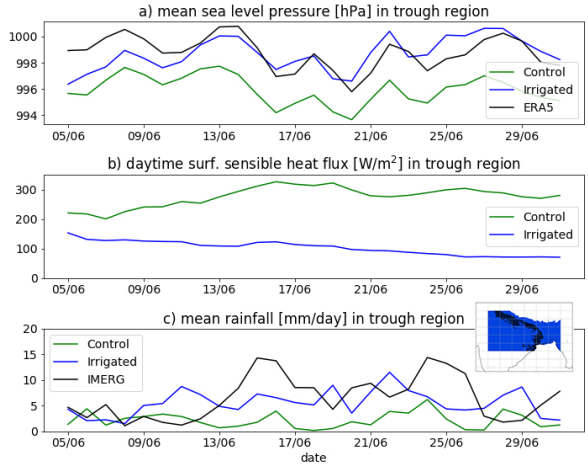

FIGURE 3 Time series of daily mean values for the monsoon trough region in the long simulations. Panel (b) shows sensible heat fluxes averaged from 06:00-18:00 local time only.Inset map shows the region over which the averaging was done in blue, with the irrigated region in dark blue.

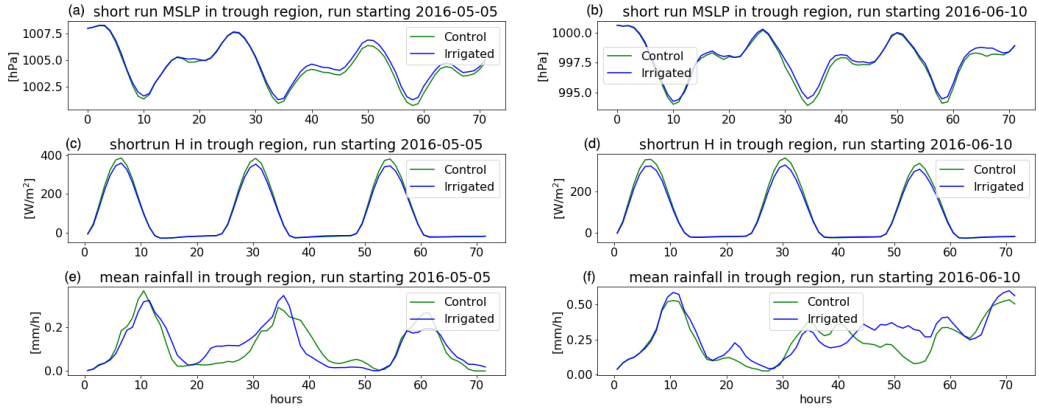

FIGURE 4 Time series of half-hourly values for the monsoon trough region in two selected examples of the short simulations. The region over which the averaging is calculated is the same as in Fig. 3.

pronounced due to both the shorter integration times – as discussed above, the circulation response timescale is on the order of five days – and, probably more importantly, the weaker forcing (compare Fig.2a to Fig.2b). Figure 4 demonstrates how much more modest the forcing and response are in the short simulations compared to the long ones. However, this is averaged over the entire monsoon trough region; Fig. 2b shows that the most irrigated regions in the short runs have average reductions of surface sensible heat flux in excess of 80 W/m^2.

Figure 2 suggests that the effect of irrigation on rainfall is generally not highest on the irrigated regions themselves but instead on nearby mountains: the Himalayan foothills, the Meghalaya Plateau, and the mountains of Myanmar. This can be broadly discerned by comparing the location of the soil moisture forcings in the top panels of Fig.2 to the

location of the rainfall response in its bottom panels, but it is shown clearly in Section 3.3.

3.2 | The diurnal cycle

Irrigation changes not just the large scale land-sea contrast but also mesoscale contrasts between irrigated and un-irrigated regions. We expect that this change in mesoscale temperature gradients will affect the diurnal cycle of circulation and rainfall. Figure 5 shows the diurnal cycle of rainfall and circulation over the monsoon core region in the month-long simulations as well as the effect of irrigation on that diurnal cycle. In many ways irrigation acts to amplify the diurnal cycle of rainfall. In the afternoon and evening (panels c and e of Fig. 5) rainfall is concentrated on the mountains while at night and in the morning it spreads over the lowlands near the moutains (panels a and g of Fig. 5). Although a general increase in rainfall in the irrigation experiments is apparent in the vicinity of the mountains at all times of day, close inspection of the 1 mm/h contour in the right column shows that the rainfall increases are stronger over the mountains at 15 local time (LT) and 21 LT, and these increases spread over the lowlands at 03 LT and 06 LT. In particular, at 21 LT we see that there are negative rainfall anomalies on the northern and, to a lesser extent, southern edges of the mountains. This suggests that the changes brought on by the irrigation experiments ~~squeeze the evening rainfall more~~ over the mountains ~~rather than on the lowlands or the Tibetan plateau~~. In the central Himalayas (about 78 °E to 87 °E), there is very little pre-monsoon rainfall in the control simulation and a considerable increase in rainfall in the irrigation simulation. The diurnal cycle is also amplified on the east coast region of India, where increases in rainfall are seen in afternoon and evening, which is already the time of peak rainfall in the control simulations.

We further explore the effect of irrigation on the diurnal cycle by constructing Hovmöller diagrams of the mean diurnal cycle across a few select latitude and longitude bands in order to illuminate the relationship between changes in diurnal circulations and rainfall and to highlight propagation. We show the results for the short simulations because they have a stronger diurnal cycle in winds and because the irrigation perturbation is more realistic; the equivalent Hovmöller diagrams for the month-long simulations (not shown) are broadly similar.

Figure 6 shows the mean diurnal cycle across the latitude band 21-23 °N as a function of longitude. We see that the afternoon rainfall anomalies on the east coast of India in the irrigation experiments is associated with the diurnal cycle and is a shift in the location maximum morning rainfall. The main rainfall increase is within the irrigated region, and occurs in the morning when the mean rainfall peaks – i.e., the rainfall increase occurs as an amplification of the diurnal cycle – but slightly west of the usual location. We see that this amplification is associated with a westward shift of the location of easterly winds, enhancing moisture advection from the irrigated region and the Bay of Bengal. [NOTE – SWITCHING TO MEAN RAINFALL INSTEAD OF INSTANTANEOUS MEANT THAT THE CHANGE IN THE DIURNAL CYCLE PREVIOUSLY DISCUSSED IN THIS FIGURE IS NO LONGER APPARENT. I PLAN TO SHIFT THE HOVMOELLER LOCATION NORTH TO 23-25N BUT I CURRENTLY CANNOT ACCESS THE DISK WHERE THE ELEVATION DATA IS.]

Figure 7 shows ~~us~~ meridional Hovmöllers for the longitude band 90-92 °E, allowing ~~us to explore~~ the region where the rainfall increase is greatest, the Meghalaya Plateau region. The Meghalaya Plateau is the smaller of the two regions labeled "mountain" in Fig. 7d and appears dwarfed by the Himalayas, but it includes Shillong Peak at 1,962 m above sea level and the towns of Sohra (previously Cherrapunji) and Mawsynram, both of which hold global records for rainfall. This region receives ~~heavy~~ inflow of moist air from the Bay of Bengal, with orographic lifting increasing the rainfall. Fig. 7c shows that there is an orographically-driven diurnal cycle with upslope flow on both the northern and southern flanks of the plateau in the daytime. This upslope flow is stronger in the irrigation simulation, leading to an enhancement of rainfall on the peaks. The evening rainfall anomaly shifts to the lowlands at night and into the following morning, as was seen in the long experiments in Fig. 5.

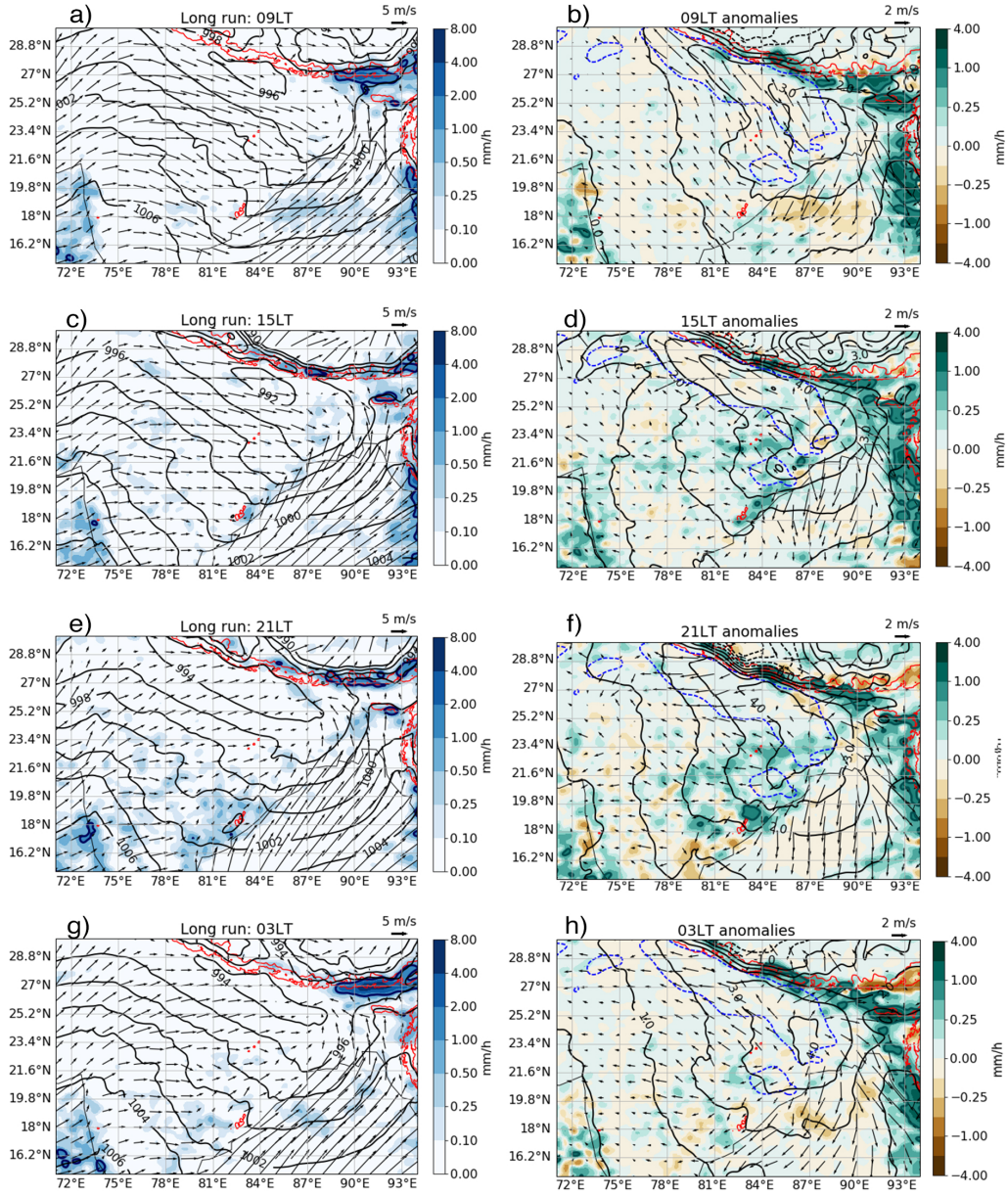

FIGURE 5 The diurnal cycle of rainfall and circulation in the long control simulation (left) and the change in the irrigation simulation (right). Red contours indicate 1000 m and 3000 m elevation and the blue contours in the right panels indicate the irrigated region as identified by a threshold mean sensible heat flux anomaly of -70 W/m^2.

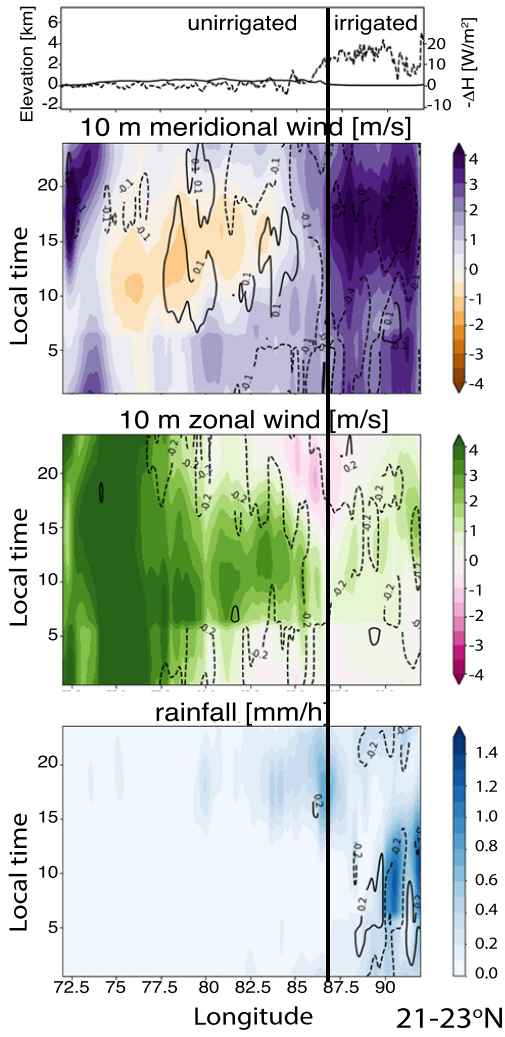

FIGURE 6 Hovmöllers of 10 m winds and rainfall averaged across the latitude band 21-23 °N, for the short simulations. Shading indicates the values for the control experiment and contours indicate the difference between irrigation and control. In the top panel, -ΔH is the mean change in surface sensible heat flux, with the sign reversed so that positive values indicate irrigated regions.

3.3 | The effect of irrigation on orographic precipitation

We confirm that irrigation has a disproportionate effect on rainfall on nearby mountains by computing the mean diurnal cycle over three land surface sub-regions within the Gangetic plain region for the short runs. These sub-regions are: the irrigated region, where the soil moisture perturbation exceeded 5 kg/m^2; the adjacent region, which is close to the irrigated region and is below 300 m elevation; and the orographic region, which is near the irrigated region and is at elevation exceeding 300 m. Figure 8 shows that the most substantial and statistically significant changes are

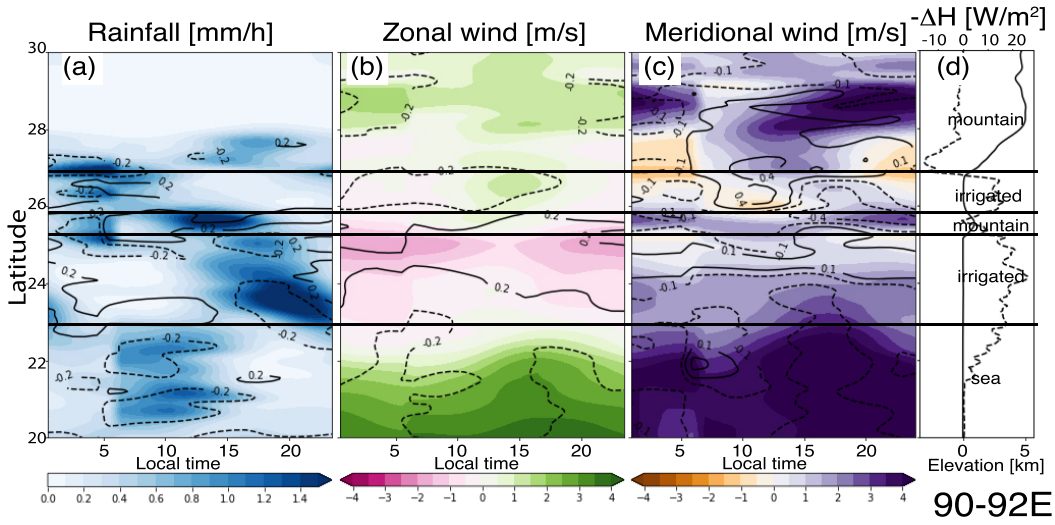

FIGURE 7 Hovmöllers of 10 m winds and rainfall averaged across the longitude band 90-92 °N, for the short simulations. Shading indicates the values for the control experiment and contours indicate the difference between irrigation and control. In panel (d), -ΔH is the mean change in surface sensible heat flux, reversed so that positive values indicate irrigated regions.

as follows: increases on the orographic region of roughly 10-30% in the daytime; decreases in the afternoon and at night over the irrigated region which are partially compensated by increases in the morning; and increases of roughly 30% in the morning on the adjacent region, largely at the base of the mountains. Because these mountainous regions are vulnerable to extreme rainfall impacts such as flash floods and landslides, we further investigate the physical mechanisms behind the changes in the subsequent section, with particular attention to the Meghalaya Plateau.

3.3.1 | The Meghalaya Plateau

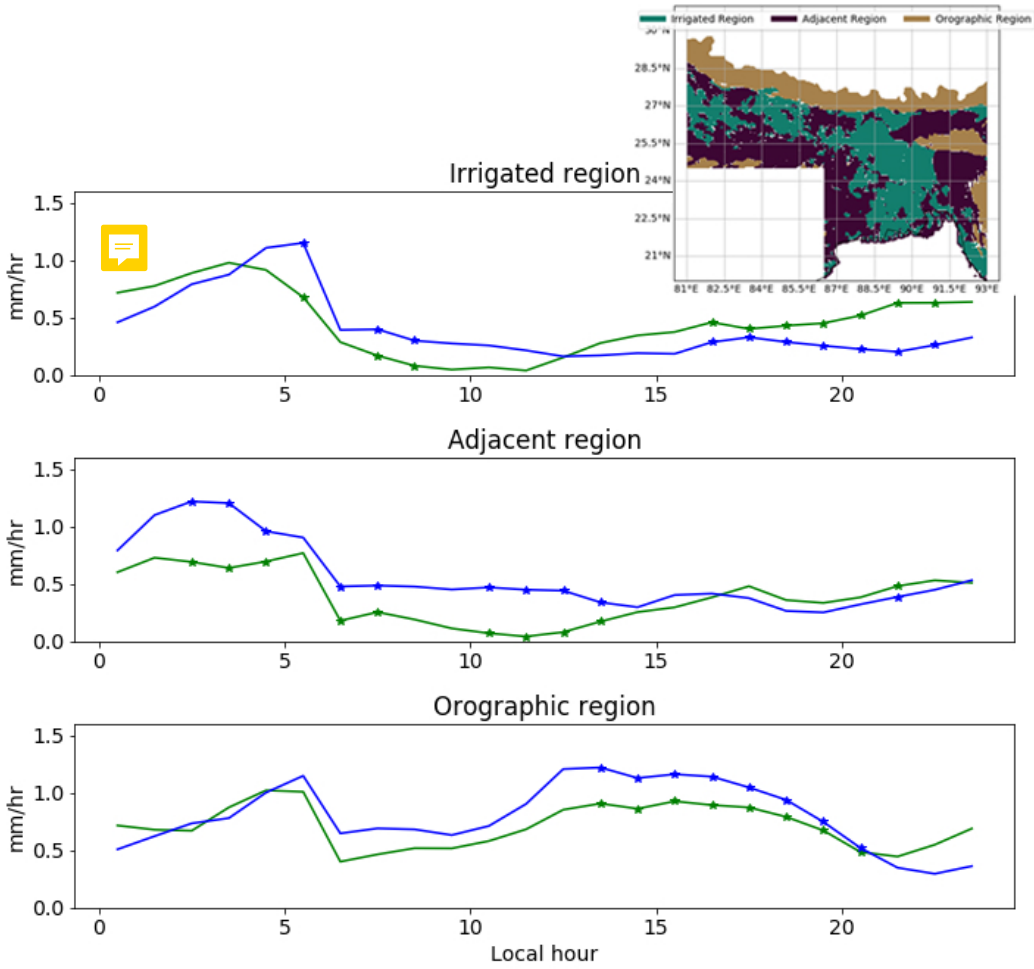

FIGURE 8 The diurnal cycle in (top) the irrigated region, identified by a change in soil moisture perturbation greater than 5 kg/m^2; regions near the irrigated region at elevation below 300 m; and (bottom) orographic regions identified as elevation greater than 300 m and slope greater than. Stars indicate that the difference between control and irrigation rainfall is statistically significant at 95% confidence using a non-parametric rank-sum test.[NEED A SHARPER VERSION OF THE INSET PLOT but currently can't access the disk where the data is]

The effect of irrigation on the diurnal cycle in the Meghalya Plateau region in the short simulations is explored in more detail in Figure 9. In the morning, rainfall is particularly enhanced on the northern flank of the plateau (Fig. 9a). In the afternoon (Fig. 9b), the rainfall increase shifts to the peaks of the plateau, and at night the anomalous rainfall shifts to the lower flanks of the plateau and the lowlands to its north and south (Fig. 9c-d).

This diurnal oscillation in the location of the rainfall anomaly can be partly understood by examining Fig. 9i-l, which show contours of virtual potential temperature ($\theta_v = T\left(\frac{p_0}{p}\right)^{\frac{R_d}{C_p}}(1+0.61r_v)$, all letters have standard meaning), with higher θ_v indicating greater buoyancy. There is a pre-existing horizontal buoyancy gradient due to the mountains, with higher buoyancy over the mountainous regions and lower buoyancy on either side because the mountains act as an elevated heat source. This gradient is enhanced during the day (Fig. 9i-j) by irrigation because the low level areas have increased evaporative cooling, which more than offsets the buoyancy increase due to higher concentrations of water vapour. Air parcels adjacent to the mountain, particularly on the northern slopes, are more buoyant relative to their surroundings in the irrigation cases than in the control cases, increasing the probability of convection. The enhanced buoyancy gradient leads to enhanced upslope flow on both the northern and southern flanks of the plateau in the afternoon (Fig. 9f), enhancing rainfall on the top of the plateau and reducing it to the south (Fig. 9b). Recall that the month-long irrigation experiment also showed the rainfall peak narrowing meridionally across the Himalayan foothills in the afternoon (Fig.5f). The anomalous buoyancy gradient in the irrigation simulations reverses sign at night (Fig. 9k-l), so that the upslope buoyancy gradient is weaker at night in the irrigated simulations than in control, especially on the southern flank of the plateau. Early in the night the rainfall anomaly is predominantly over the flanks of the plateau (Fig.9c), and it propagates north and south over the irrigated plains throughout the night and into the morning (Fig. 9d).

| Changes in mountain-valley flows

Figs 7 -9 suggest that increases in rainfall on the Meghalaya plateau and the Himalayan foothills are generally preceded by strengthened upslope flow tied to diurnally varying buoyancy gradients. We now investigate the general relationship between rainfall and upslope flow throughout the irrigated region. First we define the upslope flow parameter η:

$$\eta = \vec{u} \cdot \nabla h,$$

where $\vec{u}$ is the horizontal wind vector and h is the surface elevation. Larger positive (negative) values of η indicate flow that is more upslope (downslope). We binned η by elevation from 0 to 4000 m, with 50 m bin spacing, and by time of day, and we then averaged η from 80-92 °E and 22-29 °E. This is shown in Figure 10 along with the rainfall and 2 m θ_v which have been similarly binned and averaged.

Fig. 10a shows that what was seen in Fig. 9 for the Meghalaya region is generally true. There is a pre-existing upslope buoyancy gradient in the control simulations which is strongest during the day. In the irrigation experiments, this gradient is enhanced during the day and slightly weakened in the early morning. Similarly, there is a peak in upslope flow (Fig. 10b) during the day with downslope flow at night in the control runs. In the irrigation runs, the upslope flow change is positive on average at all times of day, so upslope flow is stronger during the day and downslope flow is weaker at night, and there is a delay in the timing of both the peak in the upslope flow and the transition from upslope to downslope flow.

There is a strong afternoon/evening peak in rainfall on elevations above about 1000 m, with a secondary peak

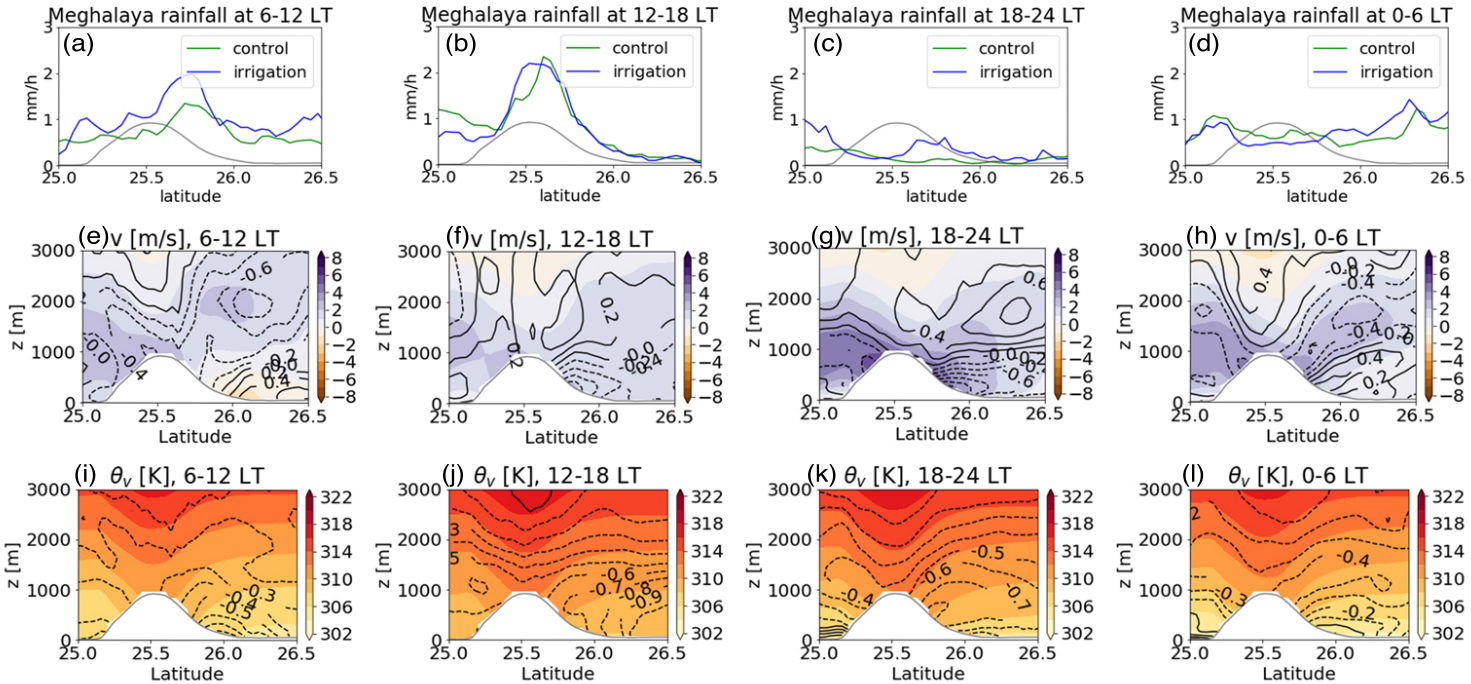

FIGURE The diurnal cycle of rainfall, meridional winds, and buoyancy in the Meghalaya region, where irrigation produced the largest rainfall increase. In a-d, the grey line indicates the mountain height (in km) to aid interpretation.

in the early mornings (Fig. 10c). In the irrigation simulations, rainfall is suppressed in the early to mid morning and enhanced in the afternoon into early night, amplifying the diurnal cycle and delaying the peak in rainfall as with upslope flow. When the irrigation-minus-control values of all three fields are combined (Fig 10d), we see that the daytime increase in upslope flow coincides with the late morning timing of the strongest increase in the upslope buoyancy gradient, and that the enhancement of orographic afternoon rainfall occurs two to three hours later. The greatest orographic rainfall increase occurs later in the evening, coinciding with the delayed shift to downslope flow and weakening of the downslope flow; this likely increases convergence on the mountain slopes. There is some suggestion that the nighttime rainfall increase on the mountains propagates down into the lowlands in the early morning and plays a role in the morning rainfall increase that occurs in the 'adjacent' region in Fig. 8b.

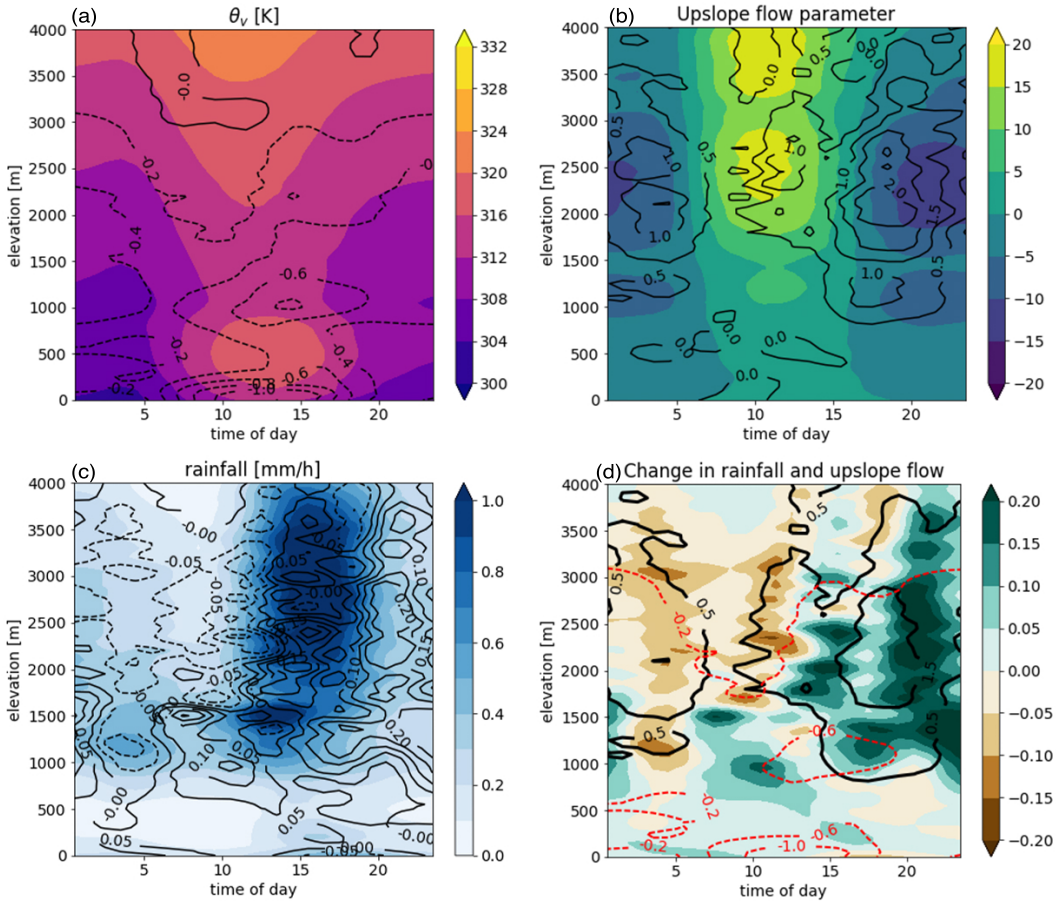

FIGURE 10 Virtual potential temperature θ_v, the upslope flow parameter η, and rainfall, binned by time of day and elevation, across the IGP region. In (a)-(c), shading shows the mean from the short control simulations while contours show the difference between irrigation and control. In (d), shading indicates the rainfall change, black contours show the upslope flow change, and red dashed contours show the change in θ_v.

Summary and conclusion

We examine the effect of realistic irrigation in the Ganges basin on pre-monsoon rainfall in convection permitting simulations. While there are many modelling studies of the effect of irrigation on the Indian monsoon, these usually use GCMs, which are known to poorly represent the response of convection to surface forcing (Taylor et al. 2013; Birch et al. 2015). By simulating the effect of irrigation on the pre-monsoon, during synoptically quiet periods, we isolate the effect of irrigation on local convection and mesoscale circulations, rather than on the effect of irrigation on the continental scale monsoon circulation. By using convection permitting simulations, we avoid the errors in land-atmosphere coupling found by (Taylor et al., 2013).

The overall effect of irrigation is to increase pre-monsoon rainfall, though this effect has considerable spatial variability. Rainfall enhancement is particularly limited by mean state humidity: much of northwestern India in the pre-monsoon is simply too dry for the moisture and circulation perturbations associated with irrigation to produce rainfall in our simulations. The greatest effect of irrigation on pre-monsoon rainfall occurs through orographic precipitation mechanisms, summarised in Figure 11. Irrigation cools the near-surface in low-lying areas, enhancing the buoyancy gradient between irrigated regions and nearby mountains. This strengthens daytime upslope flow and delays the timing of peak upslope winds, enhancing evening rainfall on the mountains. Downslope flow overnight is also weakened. The rainfall on the irrigated regions near the mountains is ~~increased most pronouncedly~~ overnight and in the early morning. Irrigated regions far from orography mostly do not see an increase in rainfall, because even on the irrigated areas the rainfall increase occurs not through the local effects of moistening the column, but through the enhanced propagation of orographic rainfall downslope in the mornings. This is demonstrated by the early morning maximum of the rainfall change on the lowlands as well as the fact that increases in rainfall in lowlands occur almost exclusively in the vicinity of mountains.

The effect of irrigation on the monsoon circulation appears to be similar to those of previous studies which used coarse-scale models with cumulus convection parameterized (Saeed et al. 2009; Puma and Cook 2010; Cook et al. 2014; Chou et al. 2018), in the sense that the monsoon trough is weaker in the irrigation experiments for both the short and long simulations. GCM studies have attributed this weaker circulation to the continental-scale cooling caused by irrigation. How~~e~~ever, in contrast to previous studies, in our simulations there is still an increase in rainfall. This could be because the rainfall response to irrigation is incorrect in previous studies due to parameterised convection ~~in those simulations responding~~ incorrectly to the surface soil moisture change. However, we suspe~~r~~ct that there is a different explanation, because previous work has shown that in the absence of strong synoptic forcing, parameterized convective rainfall tends to increase, rather than decrease, over wetter soils (Taylor et al. 2013). The fact that GCM studies have decreased rainfall under irrigation suggests that in the GCM studies the rainfall change is a consequence of two competing processes: the weakening circulation (which would decrease rainfall in the GCM) and the local convective response to enhanced soil moisture (which would increase rainfall in the GCM, possibly incorrectly), with the former dominating and leading to an overall rainfall reduction.

It is likely that the difference between our results and those of previous studies is due to the season. Based on our and others' results, we hypothesize the following: irrigation enhances pre-monsoon rainfall, which is driven primarily by local convection and mesoscale circulations, while it reduces monsoon rainfall by weakening the large scale circulation and delaying monsoon onset. This is consistent with the observational findings of Niyogi et al. (2010) and is plausibly consistent with the GCM findings of Chou et al. (2018), who saw a rainfall increase in some parts of South Asia in May due to irrigation despite an overall decrease in summer monsoon rainfall. This would be best explored with an ensemble of longer running convection permitting experiments which covered at least one full monsoon season.

Furthermore, previous GCM studies did not discuss the effect of irrigation on orographic precipitation. Here

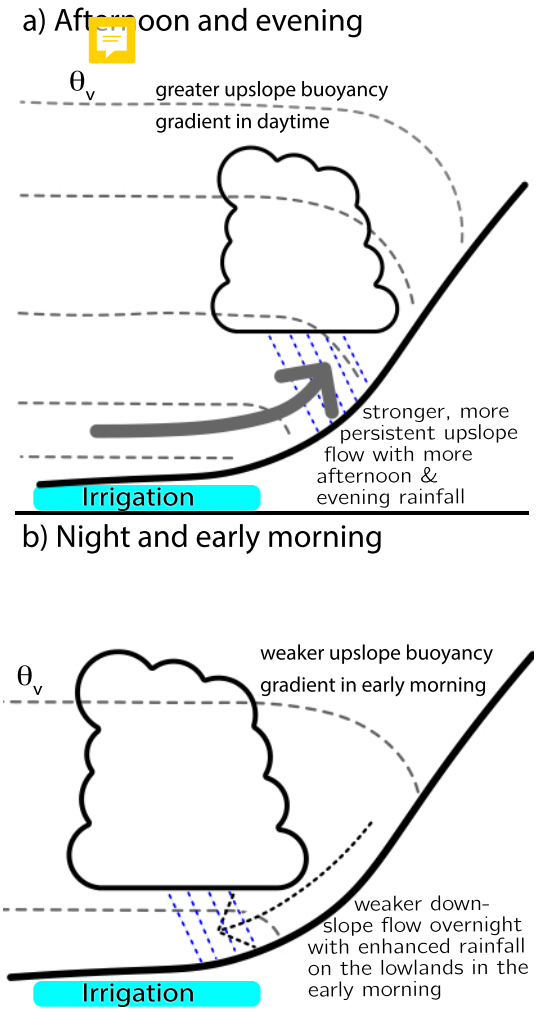

FIGURE 11 A schematic illustration of the main ways that irrigation affects pre-monsoon rainfall in convection-permitting simulations, with enhanced buoyancy-driven upslope flow in the daytime and increased rainfall on the mountain slopes; and reduced downslope flow at night and morning, with more rainfall on the lowlands.

the proper resolution of mountain-valley flows and the convective respose to those mesoscale circulation changes induced by irrigation is likely required. Chou et al. (2018) do find (but did not discuss) a rainfall increase over some mountainous areas, but these appear more to be an orographic enhancement of a general east-west tri-pole pattern in the rainfall response to irrigation (see their Fig. 3). If irrigation increases pre-monsoon orographic precipitation, it likely increases the chance of extreme rainfall leading to flash floods and landslides. This physical mechanism need not be limited to India and could in fact operate in many locations where irrigation occurs near mountain ranges, including in regions such as the Indus where irrigation was not studied in this paper.

references

Emma J. Barton, Christopher M. Taylor, Douglas J. Parker, Andrew G. Turner, Danijel Belusic, Steven J. Böing, Jennifer K. Brooke, R. Chawn Harlow, Phil P. Harris, Kieran Hunt, A. Jayakumar, and Ashis K. Mitra. A case-study of land–atmosphere coupling during monsoon onset in northern India. *Quarterly Journal of the Royal Meteorological Society*, apr 2019. doi: 10.1002/qj.3538.

H Beaudoing and M Rodell. Gldas noah land surface model l4 3 hourly 0.25× 0.25 degree v2. 1. *Goddard Earth Sciences Data and Information Services Center (GES DISC): Greenbelt, MD, USA*, 2016.

Cathryn E. Birch, Malcolm J. Roberts, Luis Garcia-Carreras, Duncan Ackerley, Michael J. Reeder, Adrian P. Lock, and Reinhard Schiemann. Sea-Breeze Dynamics and Convection Initiation: The Influence of Convective Parameterization in Weather and Climate Model Biases. *Journal of Climate*, 28(20):8093–8108, oct 2015. doi: 10.1175/jcli-d-14-00850.1.

Chihchung Chou, Dongryeol Ryu, Min-Hui Lo, Hao-Wei Wey, and Hector M. Malano. Irrigation-Induced Land–Atmosphere Feedbacks and Their Impacts on Indian Summer Monsoon. *Journal of Climate*, 31(21):8785–8801, nov 2018. doi: 10.1175/jcli-d-17-0762.1.

Benjamin I. Cook, Sonali P. Shukla, Michael J. Puma, and Larissa S. Nazarenko. Irrigation as an historical climate forcing. *Climate Dynamics*, 44(5-6):1715–1730, jun 2014. doi: 10.1007/s00382-014-2204-7.

Ellen M Douglas, Dev Niyogi, Steve Frolking, Jagadeesh Babu Yeluripati, Roger A Pielke Sr, Nivedita Niyogi, CJ Vörösmarty, and UC Mohanty. Changes in moisture and energy fluxes due to agricultural land use and irrigation in the indian monsoon belt. *Geophysical Research Letters*, 33(14), 2006.

E.M. Douglas, A. Beltrán-Przekurat, D. Niyogi, R.A. Pielke, and C.J. Vörösmarty. The impact of agricultural intensification and irrigation on land–atmosphere interactions and Indian monsoon precipitation — A mesoscale modeling perspective. *Global and Planetary Change*, 67(1-2):117–128, may 2009. doi: 10.1016/j.gloplacha.2008.12.007.

Matthieu Guimberteau, Katia Laval, Alain Perrier, and Jan Polcher. Global effect of irrigation and its impact on the onset of the Indian summer monsoon. *Climate Dynamics*, 39(6):1329–1348, dec 2011. doi: 10.1007/s00382-011-1252-5.

Hans Hersbach, Bill Bell, Paul Berrisford, Shoji Hirahara, András Horányi, Joaquín Muñoz-Sabater, Julien Nicolas, Carole Peubey, Raluca Radu, Dinand Schepers, et al. The era5 global reanalysis. *Quarterly Journal of the Royal Meteorological Society*, 146(730):1999–2049, 2020.

George J Huffman, David T Bolvin, Dan Braithwaite, Kuolin Hsu, Robert Joyce, Pingping Xie, and Soo-Hyun Yoo. Nasa global precipitation measurement (gpm) integrated multi-satellite retrievals for gpm (imerg). *Algorithm Theoretical Basis Document (ATBD) Version*, 4:26, 2015.

Kieran MR Hunt and Jennifer K Fletcher. The relationship between indian monsoon rainfall and low-pressure systems. *Climate Dynamics*, 53(3-4):1859–1871, 2019.

M. N. Islam. International Watercourses Law for the 21st Century: The Case of the River Ganges Basin. Edited by SURYA P. SUBEDI. *Journal of Environmental Law*, 19(1):143–145, aug 2006. doi: 10.1093/jel/eql027.

RD Koster, PA Dirmeyer, Z Guo, G Bonan, E Chan, P Cox, CT Gordon, S Kanae, E Kowalczyk, D Lawrence, P Liu, CH Lu, S Malyshev, B McAvaney, K Mitchell, D Mocko, T Oki, K Oleson, A Pitman, YC Sud, CM Taylor, D Verseghy, R Vasic, Y Xue, and T Yamada. Regions of strong coupling between soil moisture and precipitation. *Science*, 305:1138–40, Aug 2004.

Eungul Lee, Thomas N. Chase, Balaji Rajagopalan, Roger G. Barry, Trent W. Biggs, and Peter J. Lawrence. Effects of irrigation and vegetation activity on early Indian summer monsoon variability. *International Journal of Climatology*, 29(4):573–581, mar 2009. doi: 10.1002/joc.1721.

Gill M. Martin, Malcolm E. Brooks, Ben Johnson, Sean F. Milton, Stuart Webster, A. Jayakumar, Ashis K. Mitra, D. Rajan, and Kieran M. R. Hunt. Forecasting the monsoon on daily to seasonal time-scales in support of a field campaign. *Quarterly Journal of the Royal Meteorological Society*, 146(731):2906–2927, 2020. doi: https://doi.org/10.1002/qj.3620. URL https://rmets.onlinelibrary.wiley.com/doi/abs/10.1002/qj.3620.

Ashis K Mitra, AK Bohra, MN Rajeevan, and TN Krishnamurti. Daily indian precipitation analysis formed from a merge of rain-gauge data with the trmm tmpa satellite-derived rainfall estimates. *Journal of the Meteorological Society of Japan. Ser. II*, 87:265–279, 2009.

Dev Niyogi, Chandra Kishtawal, Shivam Tripathi, and Rao S Govindaraju. Observational evidence that agricultural intensification and land use change may be reducing the indian summer monsoon rainfall. *Water Resources Research*, 46(3), 2010.

M. J. Puma and B. I. Cook. Effects of irrigation on global climate during the 20th century. *Journal of Geophysical Research*, 115 (D16), aug 2010. doi: 10.1029/2010jd014122.

M Rajeevan, Sulochana Gadgil, and Jyoti Bhate. Active and break spells of the indian summer monsoon. *Journal of earth system science*, 119(3):229–247, 2010.

Matthew Rodell, PR Houser, UEA Jambor, J Gottschalck, K Mitchell, C-J Meng, K Arsenault, B Cosgrove, J Radakovich, M Bosilovich, et al. The global land data assimilation system. *Bulletin of the American Meteorological Society*, 85(3):381–394, 2004.

William J. Sacks, Benjamin I. Cook, Nikolaus Buenning, Samuel Levis, and Joseph H. Helkowski. Effects of global irrigation on the near-surface climate. *Climate Dynamics*, 33(2-3):159–175, jul 2008. doi: 10.1007/s00382-008-0445-z.

Fahad Saeed, Stefan Hagemann, and Daniela Jacob. Impact of irrigation on the South Asian summer monsoon. *Geophysical Research Letters*, 36(20), oct 2009. doi: 10.1029/2009gl040625.

Sonali P. Shukla, Michael J. Puma, and Benjamin I. Cook. The response of the South Asian Summer Monsoon circulation to intensified irrigation in global climate model simulations. *Climate Dynamics*, 42(1-2):21–36, may 2013. doi: 10.1007/s00382-013-1786-9.

Kummu M. Porkka M. Döll P. Ramankutty N. Siebert, S. and B.R. Scanlon. A global data set of the extent of irrigated land from 1900 to 2005. *Hydrology and Earth System Sciences*, 19(3), 2015.

Rachel A. Stratton, Catherine A. Senior, Simon B. Vosper, Sonja S. Folwell, Ian A. Boutle, Paul D. Earnshaw, Elizabeth Kendon, Adrian P. Lock, Andrew Malcolm, James Manners, Cyril J. Morcrette, Christopher Short, Alison J. Stirling, Christopher M. Taylor, Simon Tucker, Stuart Webster, and Jonathan M. Wilkinson. A pan-african convection-permitting regional climate simulation with the met office unified model: Cp4-africa. *Journal of Climate*, 31(9):3485 – 3508, 2018. doi: 10.1175/JCLI-D-17-0503.1. URL https://journals.ametsoc.org/view/journals/clim/31/9/jcli-d-17-0503.1.xml.

Christopher M. Taylor, Richard A. M. de Jeu, Françoise Guichard, Phil P. Harris, and Wouter A. Dorigo. Afternoon rain more likely over drier soils. *Nature*, 489(7416):423–426, sep 2012. doi: 10.1038/nature11377.

Christopher M. Taylor, Cathryn E. Birch, Douglas J. Parker, Nick Dixon, Françoise Guichard, Grigory Nikulin, and Grenville M. S. Lister. Modeling soil moisture-precipitation feedback in the Sahel: Importance of spatial scale versus convective parameterization. *Geophysical Research Letters*, 40(23):6213–6218, dec 2013. doi: 10.1002/2013gl058511.

OA Tuinenburg, RWA Hutjes, T Stacke, A Wiltshire, and P Lucas-Picher. Effects of irrigation in india on the atmospheric water budget. *Journal of Hydrometeorology*, 15(3):1028–1050, 2014.

GP Weedon, S Gomes, P Viterbo, WJ Shuttleworth, and E Blyth. H. sterle, jc adam, n. bellouin, o. boucher, m. best, creation of the watch forcing data and its use to assess global and regional reference crop evaporation over land during the twentieth century. *J. Hydrometerol*, 12:823–848, 2011.

Beth J Woodhams, Cathryn E Birch, John H Marsham, Caroline L Bain, Nigel M Roberts, and Douglas FA Boyd. What is the added value of a convection-permitting model for forecasting extreme rainfall over tropical east africa? *Monthly Weather Review*, 146(9):2757–2780, 2018.